

# Quantitative Holocene climatic reconstructions for the lower Yangtze region of China

Jianyong Li<sup>1</sup>  · John Dodson<sup>1,2</sup> · Hong Yan<sup>1</sup> · Weiming Wang<sup>3</sup> · James B. Innes<sup>4</sup> · Yongqiang Zong<sup>5,6</sup> · Xiaojian Zhang<sup>7</sup> · Qinghai Xu<sup>8</sup> · Jian Ni<sup>9</sup> · Fengyan Lu<sup>1</sup>

Received: 2 December 2016 / Accepted: 24 March 2017 / Published online: 5 April 2017  
© Springer-Verlag Berlin Heidelberg 2017

**Abstract** Quantitative proxy-based and high-resolution palaeoclimatic datasets are scarce for the lower reaches of the Yangtze River (LYR) basin. This region is in a transitional vegetation zone which is climatologically sensitive; and as a birthplace for prehistorical civilization in China, it is important to understand how palaeoclimatic dynamics played a role in affecting cultural development in the region. We present a pollen-based and regionally-averaged Holocene climatic twin-dataset for mean total annual precipitation (PANN) and mean annual temperature (TANN) covering the last 10,000 years for the LYR region. This is based on the technique of weighted averaging-partial least squares regression to establish robust calibration models for obtaining reliable climatic inferences. The pollen-based reconstructions generally show an early Holocene climatic

optimum with both abundant monsoonal rainfall and warm thermal conditions, and a declining pattern of both PANN and TANN values in the middle to late Holocene. The main driving forces behind the Holocene climatic changes in the LYR area are likely summer solar insolation associated with tropical or subtropical macro-scale climatic circulations such as the Intertropical Convergence Zone (ITCZ), Western Pacific Subtropical High (WPSH), and El Niño/Southern Oscillation (ENSO). Regional multi-proxy comparisons indicate that the Holocene variations in precipitation and temperature for the LYR region display an in-phase relationship with other related proxy records from southern monsoonal China and the Indian monsoon-influenced regions, but are inconsistent with the Holocene moisture or temperature records from northern monsoonal

---

✉ Jianyong Li  
lijy@ieecas.cn

John Dodson  
john@ieecas.cn

Hong Yan  
yanhong@ieecas.cn

Weiming Wang  
wmwang@nigpas.ac.cn

James B. Innes  
j.b.innes@durham.ac.uk

- <sup>1</sup> State Key Laboratory of Loess and Quaternary Geology, Institute of Earth Environment, Chinese Academy of Sciences, Xi'an 710075, China
- <sup>2</sup> School of Biological, Earth and Environmental Sciences, University of New South Wales, Sydney 2033, Australia
- <sup>3</sup> Key Laboratory of Economic Stratigraphy and Palaeogeography, Nanjing Institute of Geology and Palaeontology, Chinese Academy of Sciences, Nanjing 210008, China

- <sup>4</sup> Geography Department, Durham University, Durham DH1 3LE, UK
- <sup>5</sup> Department of Earth Sciences, The University of Hong Kong, Hong Kong, Special Administrative Region, China
- <sup>6</sup> Guangzhou Institute of Geography, Guangzhou 510070, China
- <sup>7</sup> School of Geographic and Oceanographic Sciences, Nanjing University, Nanjing 210093, China
- <sup>8</sup> Institute of Nihewan Archaeology, Hebei Normal University, Shijiazhuang 050024, China
- <sup>9</sup> College of Chemistry and Life Sciences, Zhejiang Normal University, Jinhua 321004, China

China and the westerly-dominated region in northwestern China. Overall, our comprehensive palaeoclimatic dataset and models may be significant tools for understanding the Holocene Asian monsoonal evolution and for anticipating its future dynamics in eastern Asia.

**Keywords** Lower Yangtze · China · Holocene · Climate · Pollen · Quantitative reconstructions

## 1 Introduction

The Yangtze River and its catchment occupy one of the largest drainage-basin systems in eastern Asian continent and act as a boundary zone of northern and southern China (e.g. Zhao and Chen 1999; Wu et al. 2012). The lower reaches of the Yangtze River (LYR) are situated in an area that is dominated by the East Asian monsoonal circulation (EAM); and the natural vegetation is warm temperate broadleaf and subtropical evergreen forests as well as transitions of these biomes (e.g. Ren and Beug 2002; Innes et al. 2014). The vegetation and environment in the LYR region would have been sensitive to even small-scale Holocene climatic as well as sea level fluctuations, due largely to its special bioclimatic locality and any marked weakening or strengthening of the EAM regime (e.g. Morrill et al. 2003; Yi et al. 2003; Zong et al. 2011). In particular, the LYR has been identified as one of the birthplaces for pre-historical Chinese civilization such as the ancient Hemudu and Liangzhu Cultures, and for rice cultivation such as the domesticated paddy *Oryza sativa*, as broadly elucidated by detailed palaeoecological and archaeological evidence obtained in earlier studies (e.g. Londo et al. 2006; Zong et al. 2007; Atahan et al. 2008; Fuller et al. 2009; Zhao et al. 2009; Li et al. 2010). As a consequence, the LYR has thus been suggested as an ideal region of interest for exploring the history of Holocene environmental, climatic, and cultural changes in eastern monsoonal China (e.g. Chen et al. 2005, 2009; Innes et al. 2009, 2014; Wang et al. 2011, 2012; Zong et al. 2007, 2011, 2012).

Quantitatively-integrated and high-resolution records of Holocene precipitation and temperature variations are rarely available in the LYR region, and the nature of Holocene climatic evolution in this region remains unclear (e.g. An 2000; Yi et al. 2003; Chen et al. 2005; Zong et al. 2006, 2011, 2012; Atahan et al. 2008; Innes et al. 2009; Shu et al. 2010). Several questions arise, including (1) has the Holocene climate evolved similarly or differently between the LYR and other EAM-affected regions of China such as northern monsoonal China? (2) What potential driving factors have possibly triggered the Holocene climatic oscillations in the LYR? (3) Have precipitation and temperature patterns behaved synchronously or asynchronously during

the course of Holocene in the LYR? (4) What was the timing and magnitude of the Holocene climatic optimum in the LYR? Making progress on these issues requires regional-scale, high-resolution, and numerical palaeoclimatic data.

Quantitative palaeoclimatological estimates using biological fossil proxies preserved in sediments provide an important avenue to develop these climatic data for comparison with regionally-averaged and temporally-detailed Holocene precipitation as well as temperature data in northern China (e.g. Xu et al. 2010; Chen et al. 2015; Li et al. 2015, 2017), the Tibetan Plateau (e.g. Shen et al. 2008; Herzschuh et al. 2009; Wang et al. 2014a, b), and many regions of Europe and North America (e.g. Seppä et al. 2009; Bartlein et al. 2011; Viau et al. 2012; Heiri et al. 2014; Mauri et al. 2015; Ladd et al. 2015), at local, regional, and continental scales. The continuous and conceptual advances in developing and improving large-scale calibration datasets and novel statistical techniques, have greatly promoted the accuracy and robustness of climatic reconstructions, with different means of transforming a variety of fossil biological assemblages into numerical estimates of past rainfall and temperature during the Holocene (e.g. Birks et al. 2010; Salonen et al. 2014; Wang et al. 2014a, b; Li et al. 2015, 2017). Such reconstructed climatic data are particularly valuable for validating climatic transient-model simulations and other independent climatic proxies comprising various geophysical, geochemical, and geoecological records from both terrestrial and marine environments worldwide (e.g. Braconnot et al. 2012; Renssen et al. 2012; Heiri et al. 2014; Li et al. 2015, 2017). In this respect, pollen data are one of the most commonly-used biological proxies for quantitative Holocene terrestrial climatic inferences at a broad scale (e.g. Seppä et al. 2009; Birks et al. 2010; Wang et al. 2014a, b; Li et al. 2017).

In view of the above, we place a key focus on reporting new, high-resolution Holocene precipitation and temperature reconstructions based on three fossil pollen sequences located within the lower Yangtze region of monsoonal China. Our main purpose is to enable a broader understanding and discussion with respect to the Holocene climate-related issues presented above regarding the LYR and monsoonal China. We further assess our pollen-based Holocene climatic reconstructions by relying upon an extensive multi-proxy comparison with a large number of either single or integrated moisture- and temperature-related proxy records from China as well as other regions of the world, such as speleothem oxygen isotope records (e.g. Fleitmann et al. 2003; Wang et al. 2005), loess-palaeosol sequences (e.g. Wang et al. 2014a, b; Li et al. 2014a, b), lake sediment cores (e.g. Shen et al. 2005; Chen et al. 2015), and climate model simulations (e.g. Jin et al. 2013; Chen et al. 2014). Moreover, the most important element of this study is to contribute improved and meaningful insights for evaluating

the role of causal forces and atmospheric circulations in driving Holocene climatic, environmental, and cultural changes as well as on forecasting their future possible dynamics in the lower Yangtze region of China.

## 2 Study area

The lower valley of the Yangtze basin is located in the eastern part of monsoonal China (Fig. 1), where the Asian monsoon dominates the climate and is characterized by warm, wet monsoon in summertime and cold, dry monsoon in wintertime, with four well-pronounced climatic seasons occurring per year. The 700 hPa atmospheric airstream lines in Fig. 1 clearly show that the lower Yangtze region is under the typical influence of the East Asian summer monsoon system, whilst northwestern and southwestern China are dominated by the westerlies and Indian summer monsoon circulation, respectively. Mean annual temperature (TANN) varies between 14.5 and 16.2 °C, and mean total

annual precipitation (PANN) ranges from 800 to 1400 mm, with its maximum level taking place in July (e.g. Yi et al. 2006; Li et al. 2012). The area of our investigation is naturally covered by a high-density of water-bodies including lakes, peats, bogs, marshes, swamps and wetlands, and it has thus been particularly attractive for palaeoenvironmental studies (e.g. Tao et al. 2006; Innes et al. 2009, 2014; Wang et al. 2011, 2012). The vegetation of the LYR area is a biogeographical ecotone consisting of mixed broad leaved deciduous and evergreen forests with distinct transitional characteristics (e.g. Wu 1983; Huang and Zhang 2000). The main temperate components comprise species of *Betula*, *Ulmus*, *Alnus*, *Populus*, *Quercus*, and *Acer*. The dominant evergreen components include *Castanopsis*, *Cyclobalanopsis*, *Lithocarpus*, and Fagaceae. In addition, a low number of coniferous plant taxa such as *Pinus*, *Picea*, and Cupressaceae occur in the high-elevation mountainous areas (e.g. Zong et al. 2011, 2012). It is therefore likely that in the transitional vegetation belt of the LYR, the Holocene climatic variability would have caused a northward or southward shift of the temperate or subtropical biome because of fluctuations in precipitation as well as temperature controlled primarily by the overall variability of Eastern Asian summer monsoonal (EASM) intensity (e.g. Yi et al. 2006; Zong et al. 2007, 2011).

## 3 Materials and methods

Pollen-based quantitative estimates for both PANN and TANN were prepared from three Holocene pollen datasets at Chaohu (Chen et al. 2009), Gucheng (Yang et al. 1996), and Pingwang (Innes et al. 2014), that lie within the lower reaches of the Yangtze catchment (Fig. 1). These fossil pollen profiles were selected as they have reliable chronological control and fine-scale temporal resolution (see Table 1 for other details). The AMS radiocarbon technique was utilized to create geochronological datasets (Yang et al. 1996; Chen et al. 2009; Innes et al. 2014). Plant macrofossils, shell fragments, pollen residues, charcoal particles, and basal peats have been used for AMS dating (Yang et al. 1996; Chen et al. 2009; Innes et al. 2014). The age–depth models were estimated by a linear interpolation between adjacent samples (Yang et al. 1996; Chen et al. 2009; Innes et al. 2014). The radiocarbon dates were calibrated and

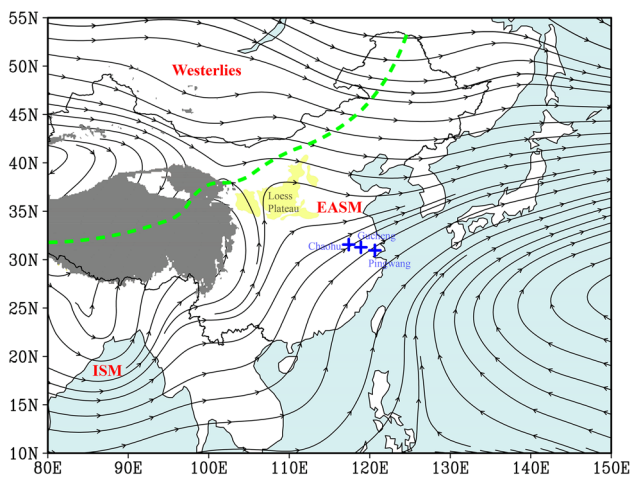


**Fig. 1** Mean 700 hPa atmospheric airstream lines between June and August based on the NCEP/NCAR Reanalysis data during the time interval of 1971–2000 (Kalnay et al. 1996). Blue plus signs correspond to the localities of three fossil sites (Chaohu, Gucheng, and Pingwang) in the lower reaches of the Yangtze basin. ISM, EASM, and Westerlies indicate the regions dominated by the Indian and Eastern Asian summer monsoon, as well as westerly air circulation, respectively. Green dashed line shows the present-day northern boundary of the Asian summer monsoon system modified from Chen et al. (2008)

**Table 1** Summary of fossil pollen datasets for PANN and TANN reconstructions at Chaohu, Gucheng and Pingwang in the lower Yangtze region of China

Site	Lat. (°)	Long. (°)	Elev. (m)	Num. dates	Res. (years)	References
Chaohu	117.39	31.56	10	10	158	Chen et al. (2009)
Gucheng	118.9	31.28	6	4	30	Yang et al. (1996)
Pingwang	120.64	30.96	1.6	5	135	Innes et al. (2014)

Lat. latitude, Long. longitude, Elev. elevation, Num. number, Res. (years) resolution (years/sample)

transformed to calendar years before present according to the IntCal13 calibration dataset (Reimer et al. 2013). The AMS  $^{14}\text{C}$  dates are presented here as cal. yr BP throughout the text. The three fossil sites are geographically very close to each other, suggesting that they have probably witnessed similar climatic histories during the Holocene.

Pollen-based numerical calibration models for both PANN and TANN were established using the Chinese surface pollen–climate database which has been shown to be robust and reliable for Holocene climatic inferences that have been described elsewhere in more detail (e.g. Zheng et al. 2008, 2014; Li et al. 2014a, b, 2015, 2017). The technique in terms of weighted averaging-partial least squares (WA-PLS; ter Braak and Juggins 1993) regression and calibration was chosen for constructing the pollen-based reconstruction models for PANN as well as TANN, because it has been successfully employed in a large number of empirical, theoretical and practical studies; and has been shown to perform as well as or better in comparison with other statistical regression approaches that are commonly applied for developing pollen-based calibration models for regional, continental and global scales (e.g. Birks 1998; Seppä et al. 2009; Birks et al. 2010; Salonen et al. 2012; Li et al. 2015, 2017). The performance of all WA-PLS models was assessed with the method of leave-one-out cross-validation (Birks 1998). The calculated model statistics for PANN and TANN embrace coefficient of determination ( $R^2$ ) between measured and predicted data, root-mean-square-error of prediction (RMSEP), and maximum bias. The two-component WA-PLS models (Fig. 2) were selected with respect to high  $R^2$ , low RMSEP and maximum bias, as well as the smallest number of useful components (Birks 1998). All terrestrial pollen taxa were taken into account and their percentage values were square-root transformed to reduce noises and stabilize variances in the pollen data (Prentice 1980). The constructions or evaluations of all WA-PLS models associated with the numerical PANN or TANN estimates were carried out using the C2 software (Juggins 2007). In addition, it has been demonstrated elsewhere that PANN and TANN are not always strongly correlated and that either PANN or TANN is statistically significant as well as ecologically meaningful in influencing broad-scale pollen distribution, indicating that they can be employed simultaneously for the pollen-based palaeoclimatic reconstructions applied here (e.g. Li et al. 2014a, b, 2015).

To obtain the underlying characteristics and summarize the potential regional signals, a total of six quantitative climatic reconstructions based on the three fossil pollen datasets were integrated to produce two general high-resolution Holocene climatic sequences (PANN and TANN) for the lower Yangtze region of China. Such a composite methodology has been successfully used for quantitative

pollen-derived and regional-scale Holocene climatic reconstructions in Europe (e.g. Seppä et al. 2009; Salonen et al. 2014; Mauri et al. 2015), North America (e.g. Viau et al. 2006, 2012; Ladd et al. 2015), and northern China (e.g. Li et al. 2015, 2017). It can be described briefly as follows. Each PANN or TANN estimate was calculated as deviations from their mean values across the Holocene. All estimated values of individual reconstructions for PANN or TANN were then combined so as to prepare two Holocene climatic records with an average time-resolution of circa 36 years for both PANN and TANN. Power spectra for potential periodicities in the pollen-stacked precipitation and temperature records were performed using the Redfit software (Schulz and Mudelsee 2002). This software is able to deal with unevenly distributed time-series data, and can test statistical significance of the spectral peaks against the red-noise background with a null-hypothesis, which can be evaluated by utilizing the first-order autoregressive signals, where characteristic time-scales as well as sampled time-spans match those of the real data, without the necessity for any interpolation (Schulz and Mudelsee 2002).

## 4 Results and discussion

### 4.1 Climatic reconstructions with low- and high-frequency trends

The pollen-inferred site-specific Holocene climatic reconstructions are presented in Fig. 3. The regionally-averaged estimates are shown in Fig. 4. Thus we provide the first ~36-year resolution pairwise-dataset for both PANN and TANN records covering the last 10,000 years. These portray both general patterns as well as detailed features of the Holocene rainfall and temperature variations for the lower reaches of the Yangtze catchment. Power spectrum analyses conducted for the composite reconstructions reveal significant periodicities of 4000, 1190, and 116 years for PANN, and of 2500, 1190, and 116 years for TANN (Fig. 5). Some of these periodicities can also be found in other Holocene Asian monsoonal records and various solar parameters (e.g. Li et al. 1996; Laskar et al. 2004; Dykoski et al. 2005; Wang et al. 2008; Wanner et al. 2008, 2011; Zhao and Feng 2014), suggesting a possible mechanistic connection among these climatic systems.

Overall high-frequency PANN and TANN fluctuations concurrently show a maximum level between 10,000 and 7000 cal. year BP, and a generally declining pattern with strong oscillations from 7000 cal. year BP to the present-day (Fig. 4). The early to middle Holocene had high values of PANN and TANN, suggesting a warm, wet climate and a strong East Asian summer monsoon, as also demonstrated by rapidly increased sea level and possible

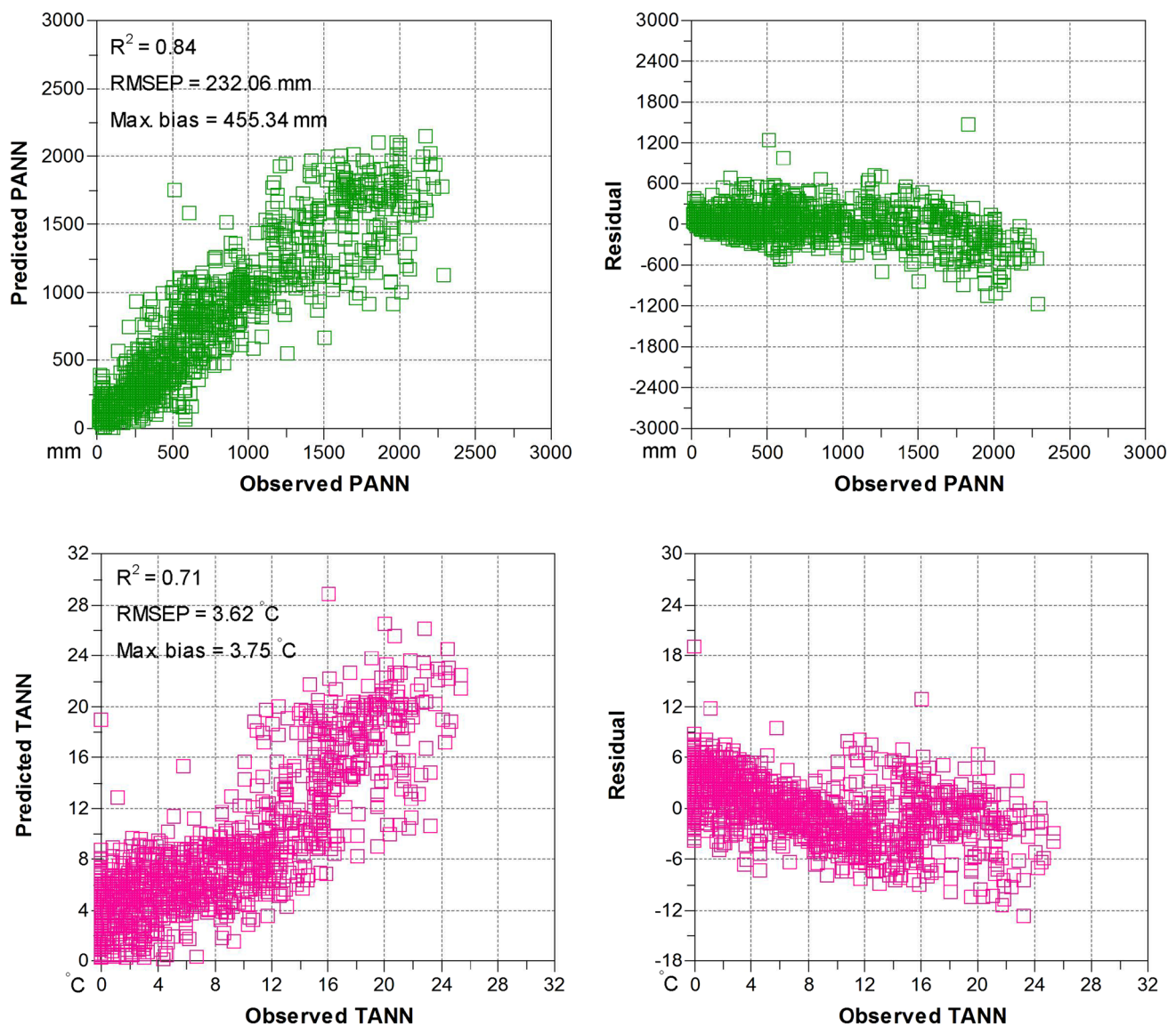


**Fig. 2** Numerical performance of the calibration models for mean total annual precipitation (PANN) as well as mean annual temperature (TANN) based on pollen data. Statistical parameters consist of

coefficient of determination ( $R^2$ ) between observed and predicted values, root-mean-square-error of prediction (RMSEP), and maximum (Max.) bias

small paddy rice cultivation in the LYR coastal plain (e.g. Innes et al. 2009; Shu et al. 2010; Zong et al. 2011; Wang et al. 2012). Subtropical forests were regarded as the dominant regional biome during this time phase, with *Castanopsis* and *Cyclobalanopsis* identified as the major tree taxa, which is evident in many published fossil pollen records from different parts of the LYR region (e.g. Chen et al. 2005; Yi et al. 2006; Innes et al. 2009; Wu et al. 2010; Li et al. 2012). However, since approximately 7000–5000 cal. year BP, the cool temperate forest elements such as *Quercus*, *Betula* and *Alnus* started to occur and expanded while subtropical elements decreased, eventually leading to a mixed temperate–evergreen

vegetation type which prevailed until modern times. The relative sea level was stable with only small fluctuations observed for this time period (e.g. Huang and Zhang 2000; Shu et al. 2007; Yi et al. 2006; Innes et al. 2014). This is closely in line with our climatic reconstructions displaying a falling trend for PANN and TANN values during this period, implying a cooling and drying climate associated with a gradually weakening EASM intensity from the middle to late Holocene in the LYR area (Fig. 4). In addition, it is noteworthy that in eastern monsoonal China, human activity played an important role in influencing vegetation cover during the late Holocene especially the last 2000 years (e.g. Zhao et al.

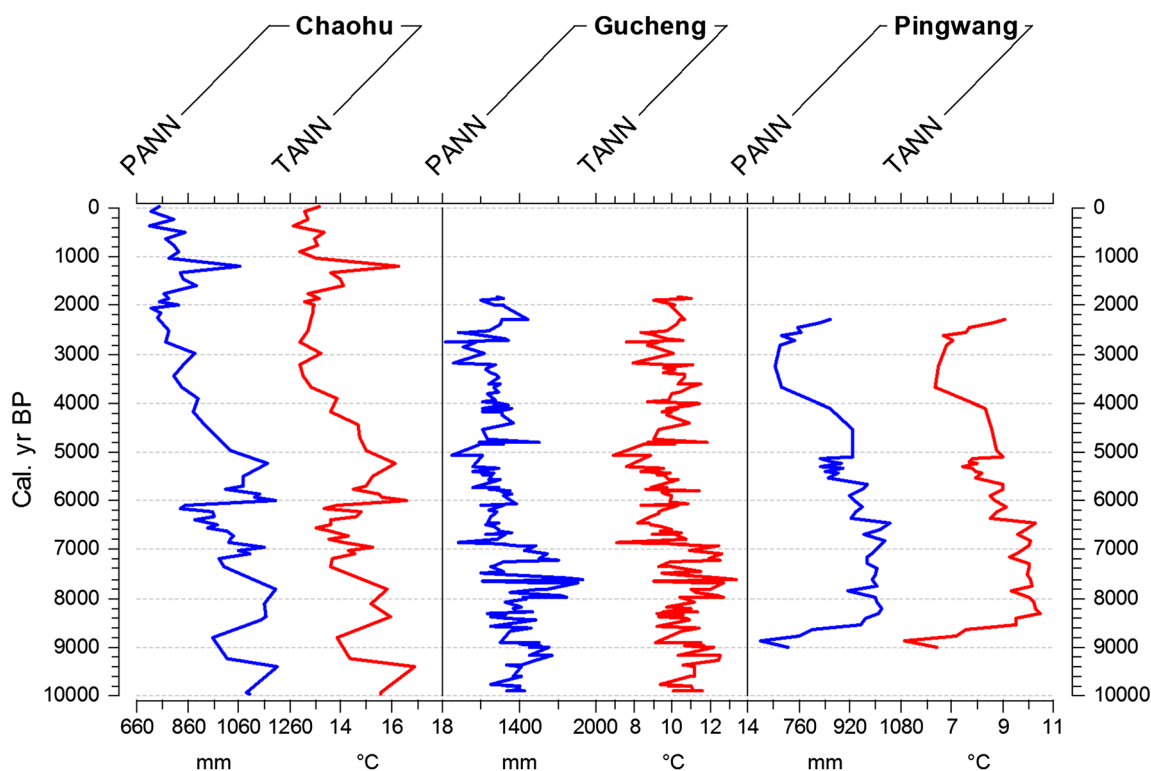


**Fig. 3** Pollen-based quantitative reconstructions for PANN with RMSEP of 232.06 mm and TANN with RMSEP of 3.62°C at Chaohu, Gucheng and Pingwang over the last 10,000 years

2009), which implies that pollen-based climatic inferences should thus be treated with caution (e.g. Li et al. 2014a, b).

Several low-frequency cooling and drying episodes can be clearly detected from our pollen-estimated PANN and TANN records. These cold and dry climatic events at about 5300, 4200, 2800 cal. year BP and during the Little Ice Age interval in the LYR region (Fig. 4) appear to be correlated well with those widely reported from other areas in China (e.g. Wang et al. 2005; Shao et al. 2006; Xu et al. 2010; Innes et al. 2014), the North Atlantic region (e.g. Bond et al. 2001; Seppä et al. 2009), and the Northern Hemisphere (e.g. Clemens 2005; Viau et al. 2006; Wanner et al. 2008, 2011). Such short-lived climatic events with high amplitude have been suggested to play a significant role in driving the demise and termination of Neolithic civilization such as the Liangzhu Culture in the Yangtze lowland area, because prehistorical farming fields and human settlements were usually situated close to water bodies such as lake shores and river channels, leading to these agricultural lands and cultural systems becoming vulnerable to abrupt changes in water supplies and thermal conditions during the Holocene, for example during the Neoglacial epoch (e.g. Zhang et al. 2005; Yao et al. 2008; Huang et al. 2010; Wu et al. 2010; Innes et al. 2014).

#### 4.2 Comparison with other subtropical or tropical Holocene records and possible mechanisms

A decadal- to centennial-scale comparison of our pollen-based PANN and TANN estimates for the LYR with other related Holocene climatic proxy records from subtropical China, the Indian summer monsoon (ISM)-influenced region and other tropical or subtropical regions of the world, indicates a macro-scale in-phase pattern of general variability, exhibiting a consistent early Holocene climatic optimum in precipitation or temperature but a relatively dryer or cooler middle to late Holocene (Fig. 6). However, it is notable that this general pattern is different to that indicated by two Holocene hydrological records from the middle reaches of the Yangtze River, that is, the mass accumulation rates of hopanoids from Dajihu peat bog as a proxy for water level, and the ratio of anhysteretic remanent magnetization (ARM) to saturation isothermal remanent magnetization (SIRM) from a stalagmite in Heshang Cave as a magnetic proxy, both suggesting a dry middle Holocene but a wetter early or late Holocene (Xie et al. 2013). These two records are also inconsistent with other proxy-based climatic records from the same region, for example, the pollen-based TANN record from Dajihu peat (Zhu et al. 2008) and the stalagmite  $\delta^{18}\text{O}$  record from Heshang

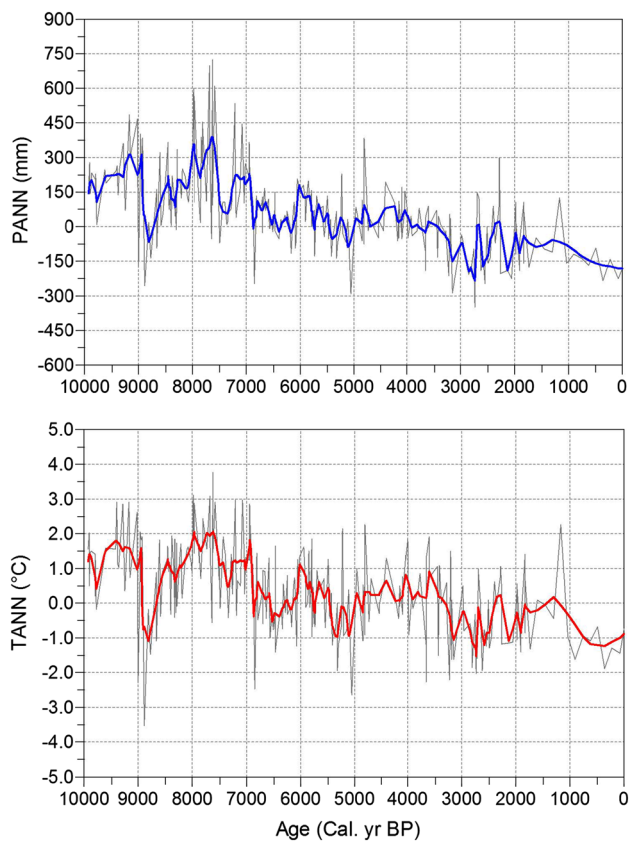


**Fig. 4** Pollen-based PANN and TANN estimates during the last 10,000 years for the lower Yangtze region of China derived from the six reconstructions in Fig. 3

Cave (Hu et al. 2008), which are in good agreement with our Holocene PANN and TANN records for the LYR. This discrepancy may result from the differences in the various reconstruction techniques, distinct temporal resolutions, reliability of sedimentary chronologies, climatic significance of diverse proxy indicators, or spatial representativeness of sampled sites (e.g. Liu et al. 2015; Rao et al. 2016; Chen et al. 2016a). In addition, the aforementioned Holocene climatic records with consistent patterns that cover a broad geographical region include the following proxy datasets: the mean summer solar insolation (Laskar et al. 2004); stalagmite  $\delta^{18}\text{O}$  records from Dongge (Dykoski et al. 2005), Sanbao (Wang et al. 2008) and Qunf (Fleitmann et al. 2003) Caves; a model-simulated PANN record for southwestern China (Chen et al. 2014); a pollen-inferred PANN estimate for Xingyun Lake in the ISM-influenced Yunan Province (Chen et al. 2014); a TANN reconstruction from Dajiuwu wetland in the EASM-dominated Hubei Province (Zhu et al. 2008); pollen-estimated moisture index (Zhao et al. 2009) as well as tree cover reconstruction (Tian et al. 2016) for southern China; a humification record from Hongyuan wetland on the southeastern Tibetan Plateau (Yu

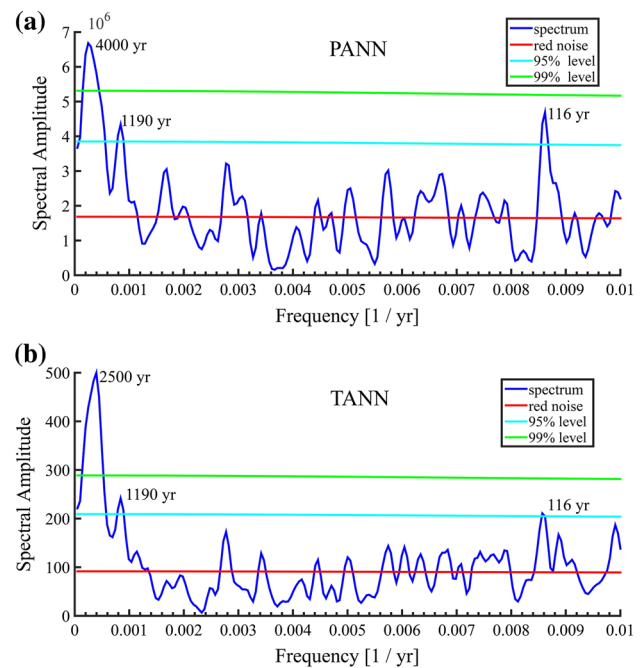


**Fig. 5** Power spectrum analyses for the pollen-stacked PANN and TANN records spanning the past 10,000 years

et al. 2006); a synthesized moisture index based on various proxy data for the southern Tibetan Plateau (Ran and Feng 2013); total organic carbon (Yancheva et al. 2007) and tree pollen records (Wang et al. 2007) from Huguangyan Maar Lake in southern China; an ISM rainfall index based on 92 monsoonal moisture records in eastern Asia (Wang et al. 2010); the Intertropical Convergence Zone (ITCZ) index inferred from Ti contents in Cariaco Basin, Venezuela (Haug et al. 2001); a *Globigerina bulloides* record from a marine sediment core in Arabian Sea (Gupta et al. 2005); composite sea surface temperature (SST) records for Western Pacific Warm Pool (WPWP; Stott et al. 2004; Koutavas and Joanides 2012); and an El Niño/Southern Oscillation (ENSO) record from Laguna Pallcacocha, Ecuador (Moy et al. 2002). Of these records, it is worth noting that the Holocene stalagmite  $\delta^{18}\text{O}$  data have been lately argued to probably represent a signal of the isotopic composition of precipitation from the ISM-influenced region rather than the EASM-dominated territory (e.g. Chen et al. 2014, 2016a; Yang et al. 2014; Wang et al. 2014a, b; Liu et al. 2015).

The above multiple lines of evidence suggest a strong causal linkage between tropical and subtropical climatic systems from the perspective of hemispheric or global scale teleconnections (Fig. 6). It has been often proposed in earlier studies that the orbitally-controlled variability of summer solar insolation would have essentially modulated and triggered the tropical and subtropical summer monsoonal

**Fig. 6** Holocene comparison of pollen-estimated **a** PANN and **b** TANN sequences for the lower Yangtze region (LYR) of China with other related climatic records including: **c** mean summer solar insolation (SI) at 65°N (Laskar et al. 2004); stalagmite  $\delta^{18}\text{O}$  series from **d** Dongge (Dykoski et al. 2005), **e** Sanbao (Wang et al. 2008), and **f** Qunf (Fleitmann et al. 2003) Caves; **g** Kiel Climate Model (KCM)-based PANN simulation for southwestern China (Chen et al. 2014); pollen-derived **h** PANN reconstruction for Xingyun Lake in Yunan Province (Chen et al. 2014) and **i** TANN reconstruction for Dajuhu wetland in Hubei Province (Zhu et al. 2008); pollen-composited **j** moisture index (MI; Zhao et al. 2009) and **k** tree cover (TC; Tian et al. 2016) records for southern China (SC); **l** humification (H) record from Hongyuan wetland on the southeastern Tibetan Plateau (Yu et al. 2006); **m** moisture index (MI) synthesized from various proxy data from the southern Tibetan Plateau (ST; Ran and Feng 2013); records of **n** total organic carbon (TOC; Yancheva et al. 2007) and **o** tree pollen percentage (TP; Wang et al. 2007) from Huguangyan Maar Lake in SC; **p** Indian summer monsoon (ISM) index synthesized for monsoonal China (Wang et al. 2010); **q** Intertropical Convergence Zone (ITCZ) index from Venezuela (Haug et al. 2001); **r** *Globigerina bulloides* percentage record from ODP Site 723 in Arabian Sea (AS; Gupta et al. 2005); **s**, **t** composite sea surface temperature (SST-1 and SST-2) records for Western Pacific Warm Pool (WPWP; Stott et al. 2004; Koutavas and Joanides 2012); and **u** El Niño/Southern Oscillation (ENSO) index from Ecuador (Moy et al. 2002). The grey band depicts the moisture or thermal maximum during the early Holocene in southern China

evolution during the post-glacial Holocene epoch (e.g. An 2000; Gupta et al. 2005; Fleitmann et al. 2003; Wang et al. 2008; Zhao et al. 2009). During the early Holocene, the high output of summer insolation may have caused the northward migration of both mean ITCZ and Western Pacific Subtropical High (WPSH) positions as indicated clearly by the high SST values in the WPWP and the Arabian Sea. This therefore resulted in a great amount of evaporated water vapor being transported from the tropical and subtropical oceanic areas to southern and eastern Asia, leading to the northward expansion and penetration of the overall summer monsoonal strength as well as its extensive rain band, and thus abundant rainfall as well as high temperature in the low-latitude regions of monsoonal Asia (e.g. Stott et al. 2004; Zhao et al. 2007; Zhou et al. 2009; Sun and Feng 2013). In contrast, during the middle to late Holocene, a reduced summer insolation would have brought about the southward retreat of both ITCZ and WPSH zones along with the decreased pattern of tropical SST values, which led to a lower moisture transportation from the ocean to continental lands, thereby causing the southward shift and weakening of the summer monsoonal intensity and its rain belt, and reduced rainfall as well as lower heat content in the southern part of monsoonal Asia and China (e.g. Dykoski et al. 2005; Wang et al. 2008; Sun and Feng 2013). In addition, an overall stepwise intensification of ENSO activity from the early to late Holocene (Fig. 6) has been suggested to bring warm water masses with higher SST to the eastern Tropical Pacific Ocean, resulting in lower SST in the western Tropical Pacific Ocean, thus progressively

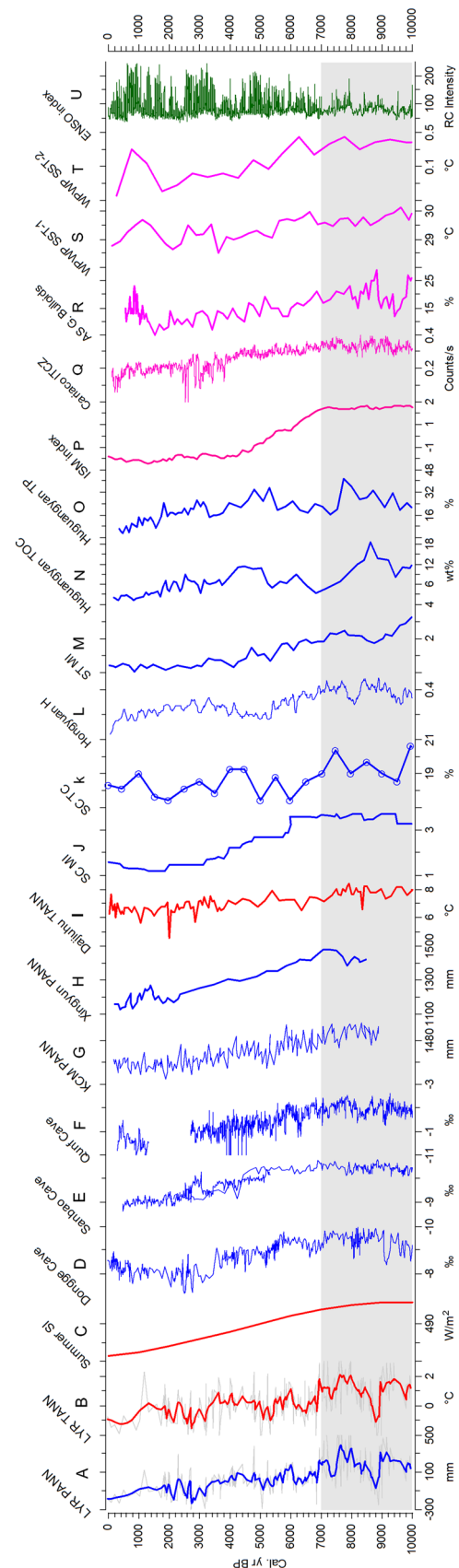


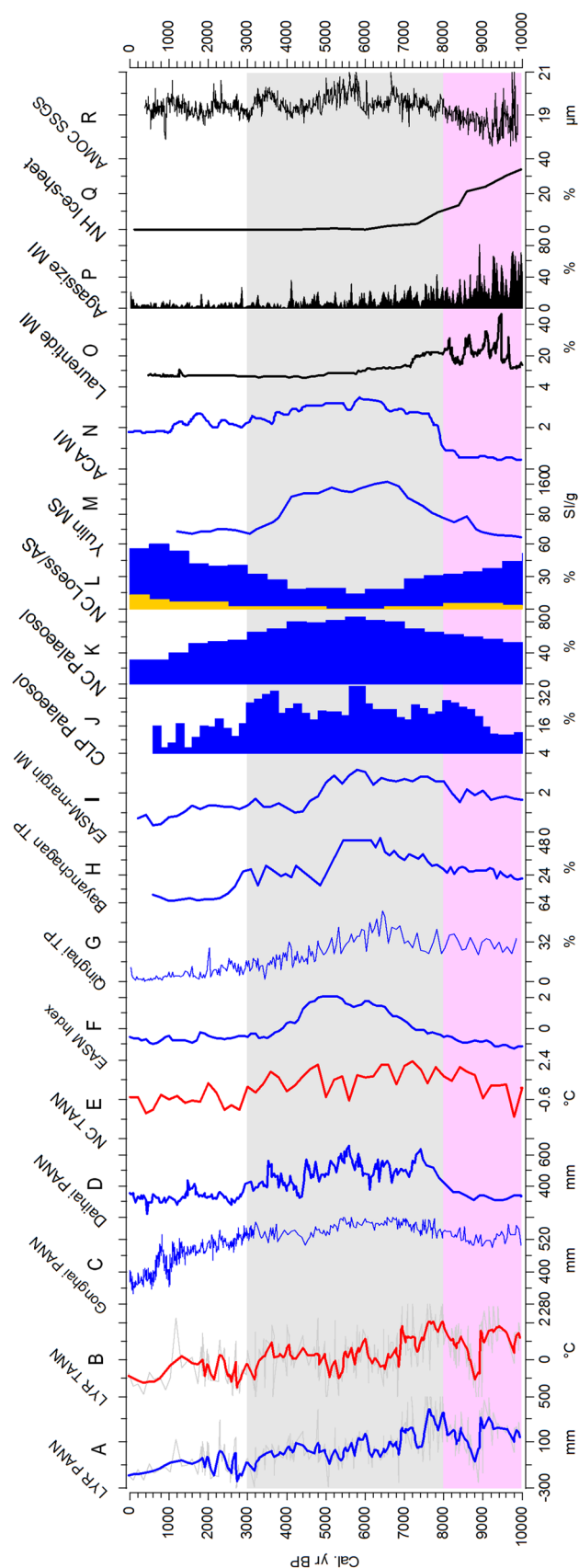


**Fig. 7** Holocene comparison of pollen-inferred **a** PANN and **b** TANN records for the lower Yangtze region (LYR) of China with other climatic proxy records for northern China and other regions of the northern Hemisphere: pollen-reconstructed PANN records for **c** Gonghai Lake (Chen et al. 2015) on the Chinese Loess Plateau (CLP) and **d** Daihai Lake (Xu et al. 2010) in northern China (NC); **e** multi-proxy-based TANN sequence for NC (Hou and Fang 2011); **f** East Asian summer monsoon (EASM) index for monsoonal China (Wang et al. 2010); tree pollen records from **g** Qinghai Lake (Shen et al. 2005) and **h** Bayanchagan Lake (Jiang et al. 2006) in NC; **i** pollen-based moisture index (MI) for the EASM marginal region (Wang and Feng 2013); frequency distributions of palaeosol occurrences in **j** CLP (Wang et al. 2014a, b) and **k** NC (Li et al. 2014a, b); **l** frequency formations of loess or aeolian sands (AS) in NC (Li et al. 2014a, b); **m** magnetic susceptibility (MS) record from the Yulin loess–palaeosol section on CLP (Lu et al. 2013); **n** moisture index (MI) synthesized for Arid Central Asia (ACA; Chen et al. 2008); melt water input (MI) from **o** the Laurentide Ice Sheet (Jennings et al. 2015) and **p** the Agassiz Ice Cap (Fisher et al. 2012); **q** ice-sheet coverage in northern Hemisphere (NH; Dyke 2004); and **r** Atlantic meridional overturning circulation (AMOC) index based on mean sortable silt grain size (SSGS) from core GS06-144 08GC in northern Atlantic Ocean (Mjell et al. 2015). The *grey band* shows the moisture or thermal maximum during the middle Holocene in northern monsoonal China. The *pink band* indicates the moisture or thermal maximum during the early Holocene in southern monsoonal China

reducing the transport of water vapor to monsoonal China during the entire Holocene (e.g. Wang et al. 2000; Higginson et al. 2004; Sun and Feng 2013).

### 4.3 Comparison with Holocene climatic records from northern monsoonal and the westerlies' region of China

A detailed comparison of our inferred precipitation and temperature reconstructions for the LYR with other high-resolution Holocene moisture and temperature records in the monsoonal regions of northern China and in the westerly-dominated areas of northwestern China, reveal an out-of-phase pattern of overall climatic shifts and a major offset in relation to timings of the Holocene climatic optimum interval (Fig. 7). These early published records consist of the following datasets: pollen-reconstructed annual rainfall series from Gonghai Lake (Chen et al. 2015) on the Chinese Loess Plateau (CLP) and Daihai Lake (Xu et al. 2010) in central Inner Mongolia; a multi-proxy based temperature reconstruction for northern China (Hou and Fang 2011); an EASM index based on various proxies in the northern part of monsoonal China (Wang et al. 2010); tree pollen percentages from Qinghai Lake (Shen et al. 2005) and Bayanchagan Lake (Jiang et al. 2006) in northern monsoonal China; a pollen-based moisture record for the northern EASM marginal region (Wang and Feng 2013); frequencies of palaeosol occurrences in the CLP (Wang et al. 2014a, b) and northern China (Li et al. 2014a, b); frequency in the formation of



loess or aeolian sands in northern China (Li et al. 2014a, b); a magnetic susceptibility record from the Yulin loess–palaeosol section on the northern CLP (Lu et al. 2013); and a moisture index synthesized from different proxy records for the westerly-influenced regions of Arid Central Asia (ACA) including northwestern China (Chen et al. 2008).

The multiple Holocene climatic records, spanning a large geographical area in both northern and northwestern China, point to an overwhelming signal with respect to a middle Holocene climatic optimum that is characterized by the highest precipitation amounts or the warmest temperature conditions (Fig. 7). Recently, Chen et al. (2016b) indicated that in the Xinjiang region as a core area of ACA, magnetic susceptibility records from four loess–palaeosol profiles have exhibited an increasing moisture pattern from the early to late Holocene. However, these trends are out-of-phase with a typical signal of an early Holocene climatic optimum demonstrated by our pollen-stacked PANN or TANN reconstructions for the LYR region as well as other Holocene monsoonal records from the subtropical and tropical domains of China or the ISM-dominated regions presented in this study (Fig. 6). Such an inconsistency may have arisen from unreliable dating controls, various proxy interpretations and resolutions, or different methodological issues and assumptions (e.g. Zhao et al. 2009; Cai et al. 2010; Sun and Feng 2013; Liu et al. 2015). In addition, the climatological viewpoints with regard to this notable timing mismatch remain under debate, which can be tentatively attributed to the significant cooling effect at a hemispherical-scale caused by the deglaciation of broad-scale remnant ice sheets in the high-latitude territories of the Northern Hemisphere during the early Holocene (Fig. 7) (e.g. Chen et al. 2008; Renssen et al. 2012; Li et al. 2015; Liu et al. 2015; Mjell et al. 2015). The rapid melting of these remnant ice sheets such as the Laurentide Ice Sheet (Jennings et al. 2015) in North America and the Agassiz Ice Cap (Fisher et al. 2012) in Greenland, would have likely yielded a large body of freshwater discharge into the northern Atlantic Ocean (Fig. 7). This may have resulted in a suppressed Atlantic meridional overturning circulation (AMOC) as well as North Atlantic Deep Water circulation (NADW), and at the same time increased Ice-Rafted Debris (IRD) in ocean sediments, massive glacial advances, strong meridional temperature gradient and westerly airstreams, and intensified Siberian High and winter monsoon strength, which may in turn have played an important role in blocking the northward movements of the summer monsoon as well as its rainfall front to the northern part of monsoonal China during the early Holocene (Fig. 7) (e.g. Zhao et al. 2009; Chen et al. 2015; Li et al. 2015; Liu et al. 2015).

## 5 Conclusions

Here we present a pollen-based Holocene climatic dataset with a ~36-year resolution for both PANN and TANN records over the last 10,000 years for the lower reaches of the Yangtze basin in eastern monsoonal China. Our reconstructions show that precipitation and temperature have a concurrent trend of variability on a centennial- to multi-decadal timescale, implying a notable climatic pattern of moist–warm or dry–cool intervals during the Holocene. Multi-proxy comparisons indicate that regional-scale Holocene rainfall and thermal variations in the lower Yangtze area are in good agreement with other Holocene climatic records from southern monsoonal China or the ISM-dominated regions, suggesting an early Holocene climatic optimum that was characterized by high precipitation and warm conditions, and a drying or cooling climate for the middle to late Holocene. The orbitally-triggered changes of summer solar insolation and tropical or subtropical climatic circulations such as ITCZ, WPSH, and ENSO may be recognized as the important driving factors for the Holocene summer monsoon variability in the lower Yangtze region of China. Further regional inter-comparisons reveal that the LYR Holocene climatic development has been different to the Holocene moisture or thermal records from the EASM-influenced northern China and the westerly-affected northwestern China where the Holocene climatic optimum mostly took place during the middle Holocene. Overall, our pollen-based high-resolution climatic dataset may be useful for validating climate model simulations, understanding the nature of monsoon climate, and predicting future climatic scenarios in monsoonal Asia and its surrounding areas. Clearly, more case studies would enhance understanding the nature of Holocene climatic changes in different bioclimatic regions of monsoonal China.

**Acknowledgements** This work was financially funded by projects from the State Key Laboratory of Loess and Quaternary Geology in the Institute of Earth Environment of the Chinese Academy of Sciences (Y652001589), the West Light Foundation of The Chinese Academy of Sciences (XAB2016B01), the National Science Foundation of China (NSFC 41522305 and 41403018), other projects from the Chinese Academy of Sciences (QYZDB-SSW-DQC001 and 132B61KYSB20160003), and Qingdao National Laboratory for Marine Science and Technology of China (QNL2016ORP0202).

## References

- An ZS (2000) The history and variability of the East Asian paleomonsoon climate. *Quat Sci Rev* 19:171–187
- Atahan P et al (2008) Holocene-aged sedimentary records of environmental changes and early agriculture in the lower Yangtze, China. *Quat Sci Rev* 27:556–570

- Bartlein PJ et al (2011) Pollen-based continental climate reconstructions at 6 and 21 ka: a global synthesis. *Clim Dyn* 37:775–802
- Birks HJB (1998) Numerical tools in palaeolimnology: progress, potentialities, and problems. *J Paleolimnol* 20:307–332
- Birks HJB, Heiri O, Seppä H, Bjune AE (2010) Strengths and weaknesses of quantitative climate reconstructions based on late-Quaternary biological proxies. *Open Ecol J* 3:68–110
- Bond G, Kromer B, Beer J, Muscheler R, Evans MN, Showers W, Hoffmann S, Lotti-Bond R, Hajdas I, Bonani G (2001) Persistent solar influence on North Atlantic climate during the Holocene. *Science* 278:1257–1266
- Braconnot P, Harrison S, Kageyama M, Bartlein J, Masson V, Abe-Ouchi A, Otto-Bliesner B, Zhao Y (2012) Evaluation of climate models using palaeoclimatic data. *Nat Clim Change* 2:417–424
- Cai YJ, Tan LC, Cheng H, An ZS, Edwards RL, Kelly MJ, Kong XG, Wang XF (2010) The variation of summer monsoon precipitation in central China since the last deglaciation. *Earth Planet Sci Lett* 291:21–31
- Chen Z, Wang Z, Schneiderman J, Tao J, Cai Y (2005) Holocene climate fluctuations in the Yangtze delta of eastern China and the Neolithic response. *Holocene* 15:915–924
- Chen FH et al (2008) Holocene moisture evolution in arid central Asia and its out-of-phase relationship with Asian monsoon history. *Quat Sci Rev* 27:351–364
- Chen W, Wang W, Dai X (2009) Holocene vegetation history with implications of human impact in the Lake Chaohu area, Anhui Province, East China. *Veget Hist Archaeobot* 18:137–146
- Chen FH, Chen XM, Chen JH, Zhou AF, Wu D, Tang LY, Zhang XJ, Huang XZ, Yu JQ (2014) Holocene vegetation history, precipitation change and Indian summer monsoon evolution documented by Xingyun Lake, Southwest China. *J Quat Sci* 29:661–674
- Chen FH et al (2015) East Asian summer monsoon precipitation variability since the last deglaciation. *Sci Rep* 5:11186
- Chen FH, Wu D, Chen JH, Zhou AF, Yu JQ, Shen J, Wang SM, Huang XZ (2016a) Holocene moisture and East Asian summer monsoon evolution in the northeastern Tibetan Plateau recorded by Lake Qinghai and its environs: A review of conflicting proxies. *Quat Sci Rev* 154:111–129
- Chen FH, Jia J, Chen JH, Li GQ, Zhang XJ, Xie HC, Xia DS, Huang W, An CB (2016b) A persistent Holocene wetting trend in arid central Asia, with wettest conditions in the late Holocene, revealed by multi-proxy analyses of loess-paleosol sequences in Xinjiang, China. *Quat Sci Rev* 146:134–146
- Clemens SC (2005) Millennial-band climate spectrum resolved and linked to centennial-scale solar cycles. *Quat Sci Rev* 24:521–531
- Dyke AS (2004) An outline of North American deglaciation with emphasis on central and northern Canada. *Dev Quat Sci* 2:373–424
- Dykoski CA, Edwards RL, Cheng H, Yuan DX, Cai YJ, Zhang ML, Lin YS, Qing JM, An ZS, Revenaugh J (2005) A high-resolution, absolute-dated Holocene and deglacial Asian monsoon record from Dongge Cave, China. *Earth Planet Sci Lett* 233:71–86
- Fisher D, Zheng J, Burgess D, Zdanowicz C, Kinnard C, Sharp M, Bourgeois J (2012) Recent melt rates of Canadian arctic ice caps are the highest in four millennia. *Glob Planet Change* 84–85:3–7
- Fleitmann D, Burns SJ, Mudelsee M, Neff U, Kramers J, Mangini A, Matter A (2003) Holocene forcing of the Indian monsoon recorded in a stalagmite from southern Oman. *Science* 300:1737–1739
- Fuller DQ, Qin L, Zheng Y, Zhao Z, Chen X, Hosoya LA, Sun GP (2009) The domestication process and domestication rate in rice: spikelet bases from the lower Yangtze. *Science* 323:1607–1610
- Gupta AK, Das M, Anderson DM (2005) Solar influence on the Indian summer monsoon during the Holocene. *Geophys Res Lett* 32:L17703
- Haug GH, Hughen KA, Sigman DM, Peterson LC, Röhl U (2001) Southward migration of the Intertropical Convergence Zone through the Holocene. *Science* 293:1304–1308
- Heiri O et al (2014) Validation of climate model-inferred regional temperature change for late-glacial Europe. *Nat Commun* 5:4914
- Herzschuh U, Kramer A, Mischke S, Zhang CJ (2009) Quantitative climate and vegetation trends since the late glacial on the northeastern Tibetan Plateau deduced from Koucha Lake pollen spectra. *Quat Res* 71:162–171
- Higginson MJ, Altabet MA, Lauren W, Herbert TD, Murray DW (2004) A solar (irradiance) trigger for millennial-scale abrupt changes in the southwest monsoon? *Paleoceanography* 19:77–100
- Hou GL, Fang X (2011) Characteristics analysis and synthetical reconstruction of regional temperature series of the Holocene in China. *J Palaeogeogr* 14:243–252 (Chinese)
- Hu CY, Henderson GM, Huang JH, Xie SC, Sun Y, Johnson KR (2008) Quantification of Holocene Asian monsoon rainfall from spatially separated cave records. *Earth Planet Sci Lett* 266:221–232
- Huang F, Zhang M (2000) Pollen and phytolith evidence for rice cultivation during the Neolithic at Longqiuzhuang, eastern Jianghuai, China. *Veget Hist Archaeobot* 9:161–168
- Huang CC, Pang J, Zha XC, Zhou Y, Su H, Li Y (2010) Extraordinary floods of 4100–4000 a BP recorded at the Late Neolithic ruins in the Jinghe River Gorges, middle reach of the Yellow River, China. *Palaeogeogr Palaeoclimatol Palaeoecol* 289:1–9
- Innes JB, Zong Y, Chen Z, Chen C, Wang Z, Wang H (2009) Environmental history, palaeoecology and human activity at the early Neolithic forager/cultivator site at Kuahuqiao, Hangzhou, eastern China. *Quat Sci Rev* 28:2277–2294
- Innes JB, Zong Y, Wang Z, Chen Z (2014) Climatic and palaeoecological changes during the mid- to late Holocene transition in eastern china: high-resolution pollen and non-pollen palynomorph analysis at Pingwang, Yangtze coastal lowlands. *Quat Sci Rev* 99:164–175
- Jennings A, Andrews J, Pearce C, Wilson L, Olfasdottir S (2015) Detrital carbonate peaks on the Labrador shelf, a 13–7 ka template for freshwater forcing from the Hudson Strait outlet of the Laurentide Ice Sheet into the subpolar gyre. *Quat Sci Rev* 107:62–80
- Jiang W, Guo Z, Sun X, Wu H, Chu G, Yuan B, Hatté C, Guiot J (2006) Reconstruction of climate and vegetation changes of Lake Bayanchagan (Inner Mongolia): Holocene variability of the East Asian monsoon. *Quat Res* 65:411–420
- Jin LY, Schneider B, Park W, Latif M, Khon V, Zhang XJ (2013) The spatial-temporal patterns of Asian summer monsoon precipitation in response to Holocene insolation change: a model-data synthesis. *Quat Sci Rev* 85:47–62
- Juggins S (2007) C2 Version 1.5 User guide. Software for ecological and palaeoecological data analysis and visualisation. Newcastle University, Newcastle upon Tyne
- Kalnay E, Kanamitsu M, Kistler R, Collins W, Deaven D, Gandin L, Iredell M, Saha S, White G, Woollen J, Zhu Y, Leetmaa A, Reynolds R (1996) The NCEP/NCAR 40-year reanalysis project. *Bull Am Meteorol Soc* 77:437–472
- Koutavas A, Joannides S (2012) El Niño-Southern Oscillation extrema in the Holocene and Last Glacial Maximum. *Paleoceanography* 27:PA4208

- Ladd M, Way RG, Viau AE (2015) The impact of using different modern climate data sets in pollen-based paleoclimate reconstructions of north America. *Quat Sci Rev* 112:78–85
- Laskar J, Robutel P, Joutel F, Gastineau M, Correia ACM, Levrard B (2004) A long term numerical solution for the insolation quantities of the Earth. *Astron Astrophys* 428:261–285
- Li KJ, Su TW, Liang HF (1996) Sunspot unit areas: a new parameter describing the long-term solar activity. *Chin Sci Bull* 49:2511–2516
- Li Y, Wu J, Hou S, Shi C, Mo D, Liu B, Zhou L (2010) Palaeoecological records of environmental change and cultural development from the Liangzhu and Qujialing archaeological sites in the middle and lower reaches of the Yangtze River. *Quat Int* 227:29–37
- Li C, Zheng Y, Yu S, Li Y, Shen H (2012) Understanding the ecological background of rice agriculture on the Ningshao plain during the Neolithic age: pollen evidence from a buried paddy field at the Tianluoshan cultural site. *Quat Sci Rev* 35:131–138
- Li JY, Zhao Y, Xu QH, Zheng Z, Lu HY, Luo YL, Li YC, Li CH, Seppä H (2014a) Human influence as a potential source of bias in pollen-based climate reconstructions. *Quat Sci Rev* 99:112–121
- Li Q, Wu H, Yu Y, Sun A, Markovic SB, Guo Z (2014b) Reconstructed moisture evolution of the deserts in northern China since the Last Glacial Maximum and its implications for the East Asian Summer Monsoon. *Glob Planet Change* 121:101–112
- Li JY et al (2015) East Asian summer monsoon precipitation variations in China over the last 9500 years: a comparison of pollen-based reconstructions and model simulations. *Holocene* 26:592–602
- Li JY et al (2017) Quantifying climatic variability in monsoonal northern China over the last 2200 years and its role in driving Chinese dynastic changes. *Quat Sci Rev* 159:35–46
- Liu JB, Chen JH, Zhang XJ, Li Y, Rao ZG, Chen FH (2015) Holocene East Asian summer monsoon records in northern China and their inconsistency with Chinese stalagmite  $\delta^{18}\text{O}$  records. *Earth Sci Rev* 148:194–208
- Londo JP, Chiang YC, Hung KH, Chiang TH, Schaal BA (2006) Phytogeography of Asian wild rice, *Oryza rufipogon*, reveals multiple independent domestications of cultivated rice, *Oryza sativa*. *Proc Natl Acad Sci USA* 103:9578–9583
- Lu HY et al (2013) Variation of East Asian monsoon precipitation during the past 21 k.y. and potential  $\text{CO}_2$  forcing. *Geology* 41:1023–1026
- Mauri A, Davis BAS, Collins PM, Kaplan JO (2015) The climate of Europe during the Holocene: a gridded pollen-based reconstruction its multi-proxy evaluation. *Quat Sci Rev* 112:109–127
- Mjell TL, Ninnemann US, Eldevik T, Kleiven HF (2015) Holocene multidecadal- to millennial-scale variations in Iceland-Scotland overflow and their relationship to climate. *Paleoceanography* 30:558–569
- Morrill C, Overpeck JT, Cole JE (2003) A synthesis of abrupt changes in the Asian summer monsoon since the last deglaciation. *Holocene* 13:465–476
- Moy CM, Seltzer GO, Rodbell DT, Anderson DM (2002) Variability of El Niño/Southern Oscillation activity at millennial time-scales during the Holocene epoch. *Nature* 420:162–165
- Prentice IC (1980) Multidimensional scaling as a research tool in Quaternary palynology: a review of theory and methods. *Rev Palaeobot Palynol* 31:71–104
- Ran M, Feng Z (2013) Holocene moisture variations across china and driving mechanisms: a synthesis of climatic records. *Quat Int* 313:179–193
- Rao ZG, Li YX, Zhang JW, Jia GD, Chen FH (2016) Investigating the long-term palaeoclimatic controls on the  $\delta\text{D}$  and  $\delta^{18}\text{O}$  of precipitation during the Holocene in the Indian and East Asian monsoonal regions. *Earth Sci Rev* 159:292–305
- Reimer PJ et al (2013) IntCal13 and Marine13 radiocarbon Age calibration curves 0–50,000 years cal BP. *Radiocarbon* 55:1869–1887
- Ren G, Beug HJ (2002) Mapping Holocene pollen data and vegetation of China. *Quat Sci Rev* 21:1395–1422
- Renssen H, Seppä H, Crosta, Goosse H, Roche DM (2012) Global characterization of the Holocene Thermal Maximum. *Quat Sci Rev* 48:7–19
- Salonen JS, Ilvonen L, Seppä H, Holmström L, Telford RJ, Gaidamavicius A, Stancikaite M, Subetto D (2012) Comparing different calibration methods (WA/WA-PLS regression and Bayesian modelling) and different-sized calibration sets in pollen-based quantitative climate reconstruction. *Holocene* 22:413–424
- Salonen JS, Luoto M, Alenius T, Heikkilä M, Seppä H, Telford RJ, Birks HJB (2014) Reconstructing palaeoclimatic variables from fossil pollen using boosted regression trees: comparison and synthesis with other quantitative reconstruction methods. *Quat Sci Rev* 88:69–81
- Schulz M, Mudelsee M (2002) REDFIT: estimating red-noise spectra directly from unevenly spaced paleoclimatic time series. *Comput Geosci* 28:421–426
- Seppä H, Bjune AE, Telford RJ, Birks HJB, Veski S (2009) Last nine-thousand years of temperature variability in Northern Europe. *Clim Past* 5:523–535
- Shao X, Wang Y, Cheng H, Kong X, Wu J, Edwards RL (2006) Long-term trend and abrupt events of the Holocene Asian monsoon inferred from a stalagmite  $\text{d}^{18}\text{O}$  record from Shennongjia in central China. *Chin Sci Bull* 51:1–8
- Shen J, Liu XQ, Wang SM, Ryo M (2005) Palaeoclimatic changes in the Qinghai Lake area during the last 18,000 years. *Quat Int* 136:131–140
- Shen CM, Liu KB, Morrill C, Overpeck JT, Peng JL, Tang LY (2008) Ecotone shift and major droughts during the mid-late Holocene in the central Tibetan Plateau. *Ecology* 89:1079–1088
- Shu JW, Wang WM, Chen W (2007) Holocene vegetation and environment changes in the NW Taihu plain, Jiangsu Province, East China. *Acta Micropalaeontol Sin* 24:210–221 (in Chinese)
- Shu JW, Wang WM, Jiang LP, Takahara H (2010) Early Neolithic vegetation history, fire regime and human activity at Kuahuqiao, Lower Yangtze River, East China: new and improved insight. *Quat Int* 227:10–21
- Stott L, Cannariato K, Thunell R, Haug GH, Koutavas A, Lund S (2004) Decline of surface temperature and salinity in the western tropical Pacific Ocean in the Holocene epoch. *Nature* 431:56–59
- Sun AZ, Feng ZD (2013) Holocene climatic reconstructions from the fossil pollen record at Qigai Nuur in the southern Mongolian Plateau. *Holocene* 23:1391–1402
- Tao J, Chen MT, Xu S (2006) A Holocene environmental record from the southern Yangtze River delta, eastern China. *Palaeogeogr Palaeoclimatol Palaeoecol* 230:204–229
- ter Braak CJF, Juggins S (1993) Weighted averaging partial least squares regression (WA-PLS): an improved method for reconstructing environmental variables from species assemblages. *Hydrobiologia* 269:485–502
- Tian F, Cao X, Dallmeyer A, Ni J, Zhao Y, Wang Y, Herzsuh U (2016) Quantitative woody cover reconstructions from eastern continental Asia of the last 22 kyr reveal strong regional peculiarities. *Quat Sci Rev* 137:33–44
- Viau AE, Gajewski K, Sawada MC, Fines P (2006) Millennial-scale temperature variability in North America during the Holocene. *J Geophys Res* 111:D09102

- Viau AE, Ladd M, Gajewski K (2012) The climate of north America during the past 2000 years reconstructed from pollen data. *Glob Planet Change* 84–85:75–83
- Wang W, Feng Z (2013) Holocene moisture evolution across the Mongolian Plateau and its surrounding areas: a synthesis of climatic records. *Earth Sci Rev* 122:38–57
- Wang B, Wu R, Fu X (2000) Pacific–East Asia teleconnection: how does ENSO affect East Asian climate? *J Clim* 13:1517–1536
- Wang Y, Cheng H, Edwards RL, He Y, Kong X, An Z, Wu J, Kelly MJ, Dykoski CA, Li X (2005) The Holocene Asian monsoon: links to solar changes and North Atlantic climate. *Science* 308:854–857
- Wang S, Lü H, Liu J, Negendank JW (2007) The early Holocene optimum inferred from a high-resolution pollen record of Huguangyan Maar Lake in southern China. *Chin Sci Bull* 52:2829–2836
- Wang YJ et al (2008) Millennial- and orbital-scale changes in the East Asian monsoon over the past 224,000 years. *Nature* 451:1090–1093
- Wang YB, Liu XQ, Herzschuh U (2010) Asynchronous evolution of the Indian and East Asian Summer Monsoon indicated by Holocene moisture patterns in monsoonal central Asia. *Earth Sci Rev* 103:135–153
- Wang Z, Li M, Zhang R, Zhuang C, Liu Y, Saito Y, Xie J, Zhao B (2011) Impacts of human activity on the late-Holocene development of the subaqueous Yangtze Delta, China, as shown by magnetic properties and sediment accumulation rates. *Holocene* 21:393–407
- Wang Z, Zhuang C, Saito Y, Chen J, Zhan Q, Wang X (2012) Early mid-Holocene sea-level change and coastal environmental response on the southern Yangtze delta plain, China: implications for the rise of Neolithic culture. *Quat Sci Rev* 35:51–62
- Wang H, Chen J, Zhang X, Chen F (2014a) Palaeosol development in the Chinese Loess Plateau as an indicator of the strength of the East Asian summer monsoon: evidence for a mid-Holocene maximum. *Quat Int* 334:155–164
- Wang Y et al (2014b) Quantitative reconstruction of precipitation changes on the NE Tibetan Plateau since the Last Glacial Maximum e extending the concept of pollen source area to pollen-based climate reconstructions from large lakes. *Clim Past* 10:21–39
- Wanner H et al (2008) Mid- to Late Holocene climate change: an overview. *Quat Sci Rev* 27:1791–1828
- Wanner H, Solomina O, Grosjean M, Ritz SP, Jetel M (2011) Structure and origin of Holocene cold events. *Quat Sci Rev* 30:3109–3123
- Wu W (1983) Holocene palaeogeography of the Hangzhou Bay. *Acta Geogr Sin* 38:113–126 (in Chinese)
- Wu L, Wang XY, Zhou KS, Mo D, Zhu C, Gao C, Zhang G, Li L, Han W (2010) Transmutations of ancient settlements and environmental changes between 6000 and 2000 a BP in the Chaohu Lake Basin, East China. *J Geogr Sci* 20:687–700
- Wu L, Li F, Zhu C, Li B (2012) Holocene environmental change and archaeology, Yangtze River Valley, China: review and prospects. *Geosci Front* 3:875–892
- Xie SC et al (2013) Concordant monsoon-driven postglacial hydrological changes in peat and stalagmite records and their impacts on prehistoric cultures in central China. *Geology* 41:827–830
- Xu QH, Xiao JL, Li YC, Tian F, Nakagawa T (2010) Pollen-based quantitative reconstruction of Holocene climate changes in the Daihai Lake area, Inner Mongolia, China. *J Clim* 23:2856–2868
- Yancheva G et al (2007) Influence of the intertropical convergence zone on the East Asian monsoon. *Nature* 445:74–77
- Yang XD, Wang SM, Tong GB (1996) Character of palynology and changes of monsoon climate over the last 10000 years in Gucheng Lake, Jiangsu Province. *Acta Bot Sin* 38:576–581 (in Chinese)
- Yang XL, Liu JB, Liang FY, Yuan DX, Yang Y, Lu YB, Chen FH (2014) Holocene stalagmite  $\delta^{18}\text{O}$  records in the East Asian monsoon region and their correlation with those in the Indian monsoon region. *Holocene* 24:1657–1664
- Yao P, Huang CC, Pang JL, Zha XC, Li XG (2008) Palaeoflood hydrological studies in the middle reaches of the Beiluohe River. *Acta Geogr Sin* 63:1198–1206 (in Chinese)
- Yi S, Saito Y, Zhao Q, Wang P (2003) Vegetation and climate changes in the Changjiang (Yangtze River) Delta, China, during the past 13,000 years inferred from pollen records. *Quat Sci Rev* 22:1501–1519
- Yi S, Saito Y, Yang DY (2006) Palynological evidence for Holocene environmental change in the Changjiang (Yangtze River) delta, China. *Palaeogeogr Palaeoclimatol Palaeoecol* 241:103–117
- Yu XF, Zhou W, Franzen LG, Feng X, Peng C, Jull AJT (2006) High-resolution peat records for Holocene monsoon history in the eastern Tibetan plateau. *Sci China Ser D. Earth Sci* 49:615–621
- Zhang Q, Zhu C, Liu CL, Jiang T (2005) Environmental change and its impacts on human settlement in the Yangtze Delta, P.R. China. *Catena* 60:267–277
- Zhao J, Chen CK (1999) *Chinese Geography* (in Chinese). Higher Education Press, Beijing
- Zhao XH, Feng XS (2014) Periodicities of solar activity and the surface temperature variation of the Earth and their correlations. *Chin Sci Bull* 59:1284–1292
- Zhao P, Zhu Y, Zhang R (2007) An Asian-Pacific teleconnection in summer tropospheric temperature and associated Asian climate variability. *Clim Dyn* 29:293–303
- Zhao Y, Yu Z, Chen F, Zhang J, Yang B (2009) Vegetation response to Holocene climate change in monsoon-influenced region of China. *Earth Sci Rev* 97:242–256
- Zheng Z et al (2008) Comparison of climatic threshold of geographical distribution between dominant plants and surface pollen in China. *Sci China Ser D. Earth Sci* 51:1107–1120
- Zheng Z et al (2014) East Asian pollen database: modern pollen distribution and its quantitative relationship with vegetation and climate. *J Biogeogr* 41:1819–1832
- Zhou X, Zhao P, Liu G (2009) Asian-Pacific Oscillation index and variation of East Asian summer monsoon over the past millennium. *Chin Sci Bull* 54:3768–3771
- Zhu C, Chen X, Zhang GS, Ma CM, Zhu Q, Li ZX, Xu WF (2008) Spore-pollen-climate factor transfer function and paleoenvironment reconstruction in Dajiuhu, Shennongjia, central China. *Chin Sci Bull* 53:42–49
- Zong Y, Lloyd JM, Leng MJ, Yim WWS, Huang G (2006) Reconstruction of Holocene monsoon history from the Pearl River estuary, southern China, using diatoms and carbon isotope ratios. *Holocene* 16:251–263
- Zong Y, Chen Z, Innes JB, Chen C, Wang Z, Wang H (2007) Fire and flood management of coastal swamp enabled first rice paddy cultivation in east China. *Nature* 449:459–462
- Zong Y, Innes JB, Wang Z, Chen Z (2011) Mid-Holocene coastal hydrology and salinity changes in the east Taihu area of the lower Yangtze wetlands, China. *Quat Res* 76:69–82
- Zong Y, Wang Z, Innes JB, Chen Z (2012) Holocene environmental change and Neolithic rice agriculture in the lower Yangtze region of China: a review. *Holocene* 22:623–635